Electronic Supporting Information

Fluorescent molecules with alternating triarylamine-substituted selenophenothiophene and triarylborane: synthesis, photophysical properties and anion sensing studies

Gulsen Turkoglu*[a] and Turan Ozturk[a,b]

[a]Department of Chemistry, Faculty of Science, Istanbul Technical University, Maslak, Istanbul 34469, Turkey

[b]TUBITAK-UME, Chemistry Group Laboratories, PO Box 54, 41471, Gebze, Kocaeli, Turkey

*Corresponding Author: gulsent06@hotmail.com

Table of Contents **Page**

1. Experimental

Materials and methods

All the solvents and chemicals were purchased from Sigma-Aldrich and Acros, which were used without further purification. Tetrahydrofuran (THF) was dried over sodium in the presence of benzophenone. All the chemical reactions were performed under N_2 atmosphere. 4,4,5,5-Tetramethyl-2-(thiophen-2-yl)-[1,3,2]dioxaborolane,[1] *N*,*N*-diphenyl-4-(4,4,5,5-tetramethyl-1,3,2-dioxaborolan-2-yl)benzeneamine,[2] 4-bromophenyldi(4-methoxyphenyl)amine[3] and *N*,*N*-bis(4-methoxyphenyl)-4-(4,4,5,5-tetramethyl-1,3,2-dioxaborolan-2-yl)benzenamine[4] were synthesized using the literature procedures. Selenopheno[3,2-*b*]thiophene (**1**) was synthesized according to our previous work.[5,6]
NMR spectra were recorded on a Varian model NMR (500 and 600 MHz). Chemical shifts were reported in ppm downfield from tetramethylsilane (TMS) for proton and carbon measurements. Mass spectra were recorded on Bruker MICROTOFQ and Thermo LCQ-Deca ion trap mass instruments. UV-Vis absorption spectra were obtained using a HITACHI U-0080D. Fluorescence spectra were conducted on HITACHI F-4500 Fluorescence Spectrophotometer. The solution fluorescence quantum yields were determined in dilute THF using Rhodamine 6G and Coumarin 6 ($\Phi_F = 0.95$ and 0.78 in ethanol, respectively) as standard substances. All the solutions used in photophysical measurements had a concentration lower than 10^{-5} M at room temperature. Cyclic voltammetry experiments were conducted using a CH-Instruments Model 400A potentiostat. All measurements were performed at a scan rate of 100 mV s^{-1} in CH_2Cl_2 solution in the presence of 0.1 M tetrabutylammonium hexafluorophosphate ($TBAPF_6$) as a supporting electrolyte at room temperature under a nitrogen atmosphere. A three-electrode configuration was used for the measurement, where platinum wires were working and counter electrodes and Ag wire was a reference electrode.

Anion sensing studies

Stock solutions of **BTPAST** and **BOMeTPAST** were prepared in THF (20 μM). For UV–Vis and fluorescence titrations, the stock solutions of F^- and CN^-, as their tetrabutylammonium salts, were prepared in THF (2 mM). The selectivity properties of the sensors were explored comparing the absorption and fluorescence spectra with the other anions such as Cl^-, Br^-, I^-, and ClO_4^- in THF.

Stoichiometry and Job plot experiment. Stoichiometry was determined by Job Plot method, which was monitored by fluorescence spectra. A series of diverse proportions of F^-/CN^- varying from 0 to 1.0 were prepared. After shaking the vials for a few minutes, emissions of the solutions were measured throughout fluorescence titration at room temperature. Mole fractions of the compounds (X), ($X_S = n_x / n_{F^-\ or\ CN^-} + n_x$), were plotted against $\Delta I.X$ ($\Delta I = I_0 - I$).[7]

Determination of binding constants. Binding constants were calculated for the formation of anion (F^-) complex with **BTPAST** and **BOMeTPAST**, applying Benesi-Hildebrand (B-H) plot (Eq. 1).[8,9]

$$\frac{1}{(I-I_o)} = \frac{1}{(I_{max}-I_o)}\left[\frac{1}{K_a[M]_o} + 1\right] \qquad \text{(Eq. 1)}$$

Where I_0 is the intensity before addition of the anion, I is the intensity in the presence of F^-/CN^-, I_{max} is the intensity upon saturation with the anion, [M] is the concentration of F^-/CN^-, and K_a is the association constant of the formed complex. The binding constants (K_a) were obtained from the intercept/slope of the B-H plot.

Limit of Detection (LoD). The detection limits of the compounds were evaluated on the basis of UV-Vis titration studies using Eq. 2.[10] Initially, a calibration curve was obtained from the plot of the absorption intensity increment, i.e. $A–A_0$, as a function of the fluoride anion concentration. The regression curve equation was thereafter reached for the low concentration part.

$$LOD = 3 \times S.D. / k \quad \text{(Eq. 2)},$$

Where S.D. stands for the standard deviation attained from the blank observations, and k is the slope obtained from the linear curve.

Synthesis

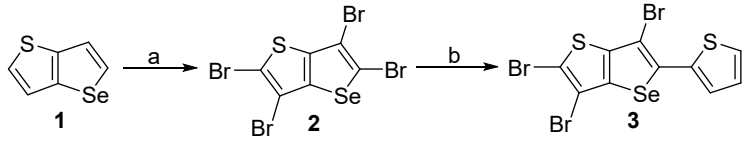

Scheme S1. Synthetic procedure for compounds **2** and **3**. Reagents/conditions: (a) Br_2, acetic acid/H_2O, 65 °C, 12h; (b) 4,4,5,5-tetramethyl-2-(thiophen-2-yl)-1,3,2-dioxaborolane, $Pd(PPh_3)_4$, K_2CO_3, THF, reflux, 24h.

2,3,5,6-Tetrabromoselenopheno[3,2-*b*]thiophene (2): To compound **1** (1.16 g 6.20 mmol) in acetic acid was added slowly bromine (1.28 mL, 24.85 mmol) at room temperature in dark. After stirring for 1 h at the same temperature, the reaction mixture was poured into water (24 mL) and stirred for 12 h at 65 °C. The precipitate was filtrated and washed with water and dried. The crude product was crystallized from THF. The product was obtained as an off-white solid in 64% yield (2.0 g); M.p. 160 °C; ^{13}C NMR (125 MHz, $CDCl_3$) δ 139.1, 134.2, 114.3, 114.2, 109.5, 109.2. MS (m/z): $[M+1]^+$ 499.

2,3,6-Tribromo-5-(thiophen-2-yl)selenopheno[3,2-b]thiophene (3): To a degassed mixture of **2** (600 mg, 1.20 mmol), 2-(thiophen-2-yl)-4,4,5,5-tetramethyl-1,3,2-dioxaborolane (300 mg, 1.43 mmol) and aqueous K_2CO_3 (4.00 mL, 2 M) in THF (40 mL) was added $Pd(PPh_3)_4$ (125 mg, 5% mol) under nitrogen atmosphere. The reaction mixture was then refluxed for 24 h, cooled to room temperature and quenched adding water and NH_4Cl (aq.). The mixture was extracted with dichloromethane, dried over anhydrous $NaSO_4$, filtered and the solvent was evaporated under reduced pressure. The crude product was purified by column chromatography over silica gel using a mixture of *n*-hexane/dichloromethane (5:1) as an eluent (R_f = 0.65) to furnish a yellow solid in 85% (512 mg) yield. M.p. 132−133 °C; ^1H NMR (500 MHz, $CDCl_3$) δ 7.43 (d, J = 5.0 Hz, 1H), 7.40 (dd, J = 3.7 and 1.0 Hz, 1H), 7.11 (dd, J = 5.0 and 3.7 Hz, 1H); ^{13}C NMR (125 MHz, $CDCl_3$) δ 141.4, 136.2, 135.8, 135.2, 127.6, 127.5, 127.3, 112.3, 109.9, 100.2; MS (m/z): $[M+1]^+$ 504.

2. Photophysical Spectra

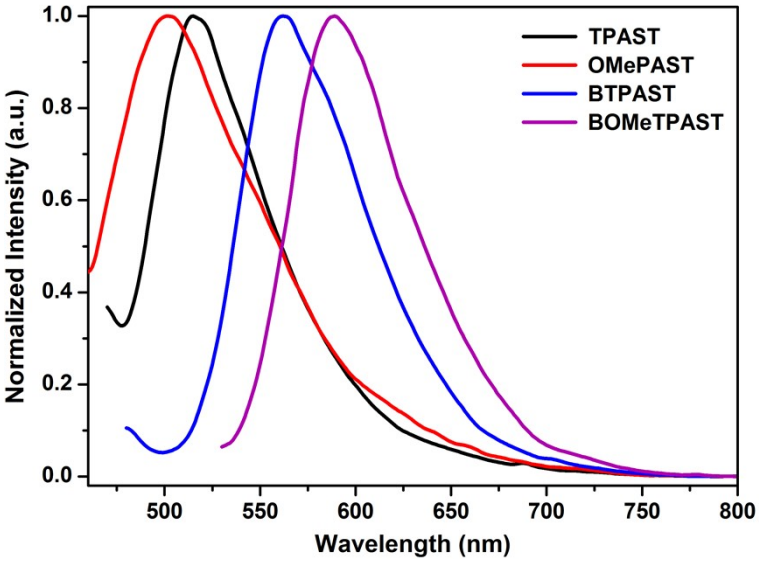

Figure S1. Emission spectra of newly synthesized compounds as spin-coating thin films. The longest-wavelength absorption maxima were used as excitation wavelengths.

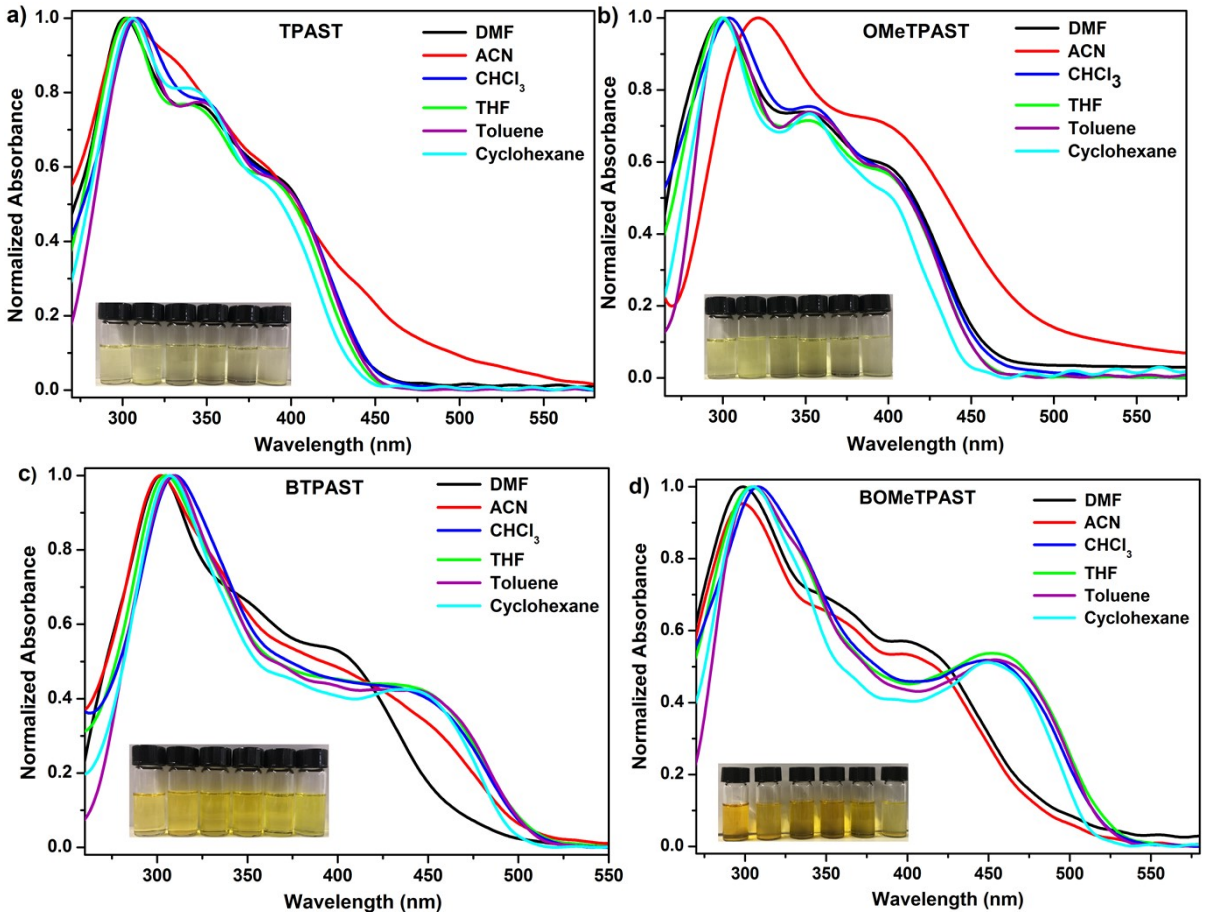

Figure S2. Apsortion spectra of compounds (a) **TPAST**, (b) **OMETPAST**, (c) **BTPAST** and (d) **BOMeTPAST** in various polarity solvents.

Tablo S1. UV-visible absorption and emission spectra of newly synthesized compounds in different solvents.

	λ_{abs} (nm)[a]				λ_{em} (nm)[a]			
Solvents	**TPAST**	**OMeTPAST**	**BTPAST**	**BOMeTPAST**	**TPAST**	**OMeTPAST**	**BTPAST**	**BOMeTPAST**
DMF	396 (s)[b]	396(s)	399	401	507	549	556	562
	345	349	351 (s)	355(s)				
ACN	386 (s)	398 (s)	417 (s)	400	497	544	608	612
	304	321	302	352				
$CHCl_3$	388 (s)	397 (s)	430	450	491	511	557	581
	345	353	309	308				
		303						
THF	393(s)	400(s)	440	455	490	512	566	595
	344	354	305	303				
Toluene	390(s)	397 (s)	443	454	494 (s)	495	540	555
	345	353	308	305	477			
Cyclohexane	386(s)	398 (s)	438	452	468	493 (s)	518	530
	336	353	372	305		475		

[a]Data were collected for solutions ([M]= $2x10^{-5}$) under air. [b]Shoulder in absorption and emission spectra.

3. Anion Binding Studies

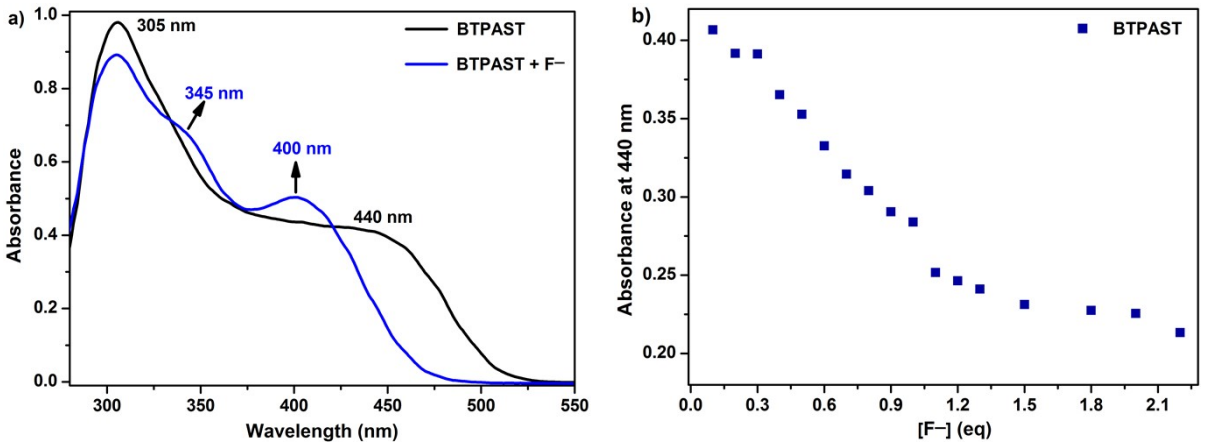

Figure S3. a) Spectral change in the absorbance of a solution **BTPAST** in THF upon the addition of TBAF (0 and 2.2 eq). b) The plot of absorbance at 440 nm as a function of [F^-].

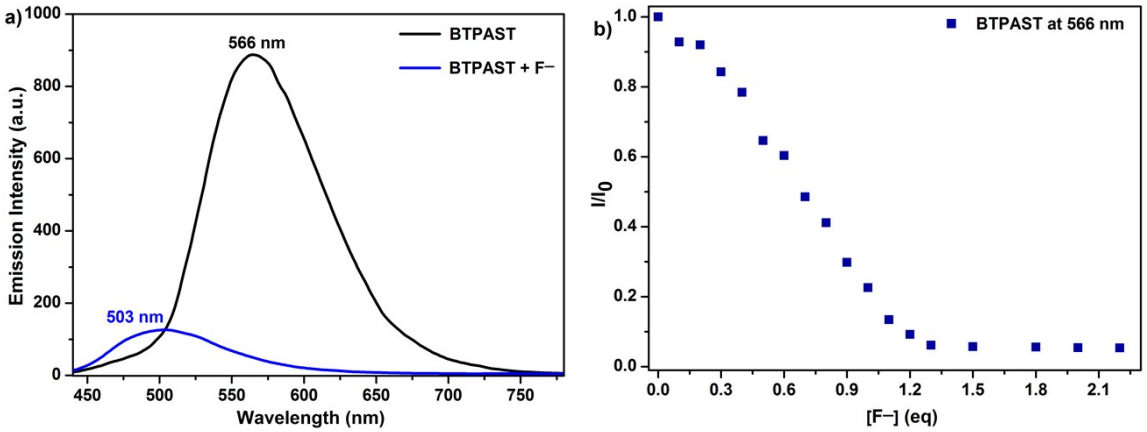

Figure S4. a) Spectral change in the emission of a solution **BTPAST** in THF upon the addition of TBAF (0 and 2.2 eq) (λ_{ex} = 440 nm). b) Stern-Volmer plots of the intensity change (I_0/I) as a function of [F^-].

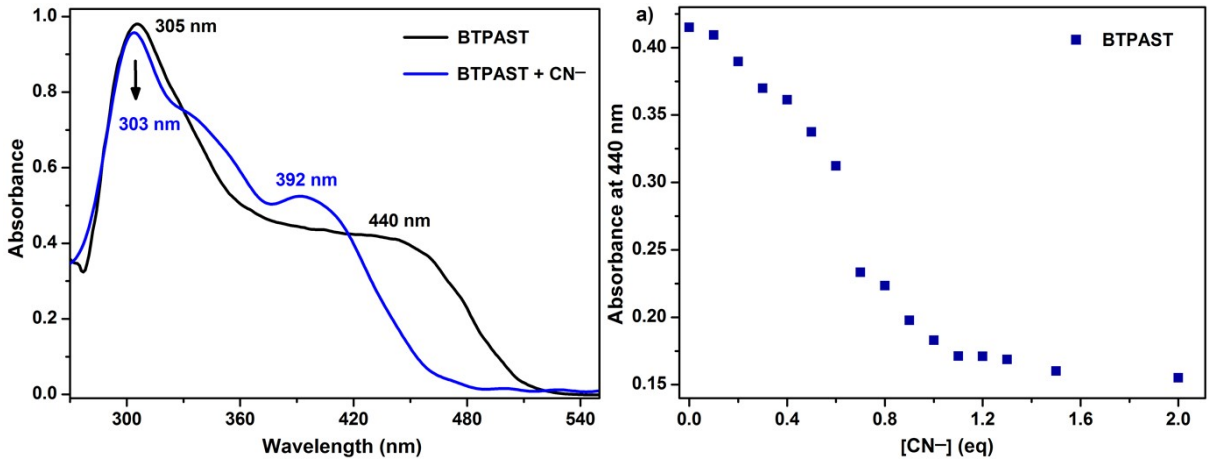

Figure S5. a) Spectral change in the absorbance of a solution **BTPAST** in THF upon the addition of TBACN (0 and 2.0 eq). b) The plot of absorbance at 440 nm as a function of [CN^-].

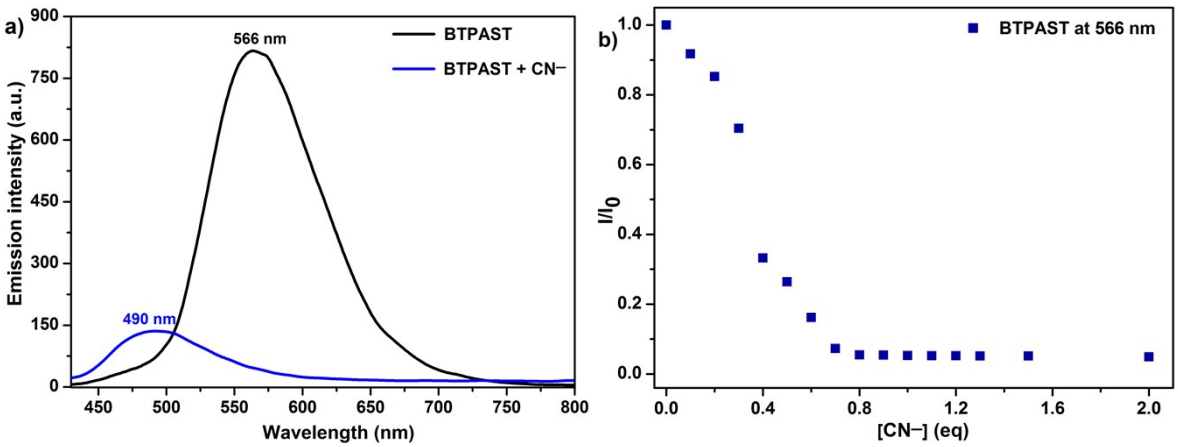

Figure S6. a) Spectral change in the emission of a solution **BTPAST** in THF upon the addition of TBACN (0 and 2.0 eq) (λ_{ex} = 440 nm). b) Stern-Volmer plots of the intensity change (I0/I) as a function of [CN−].

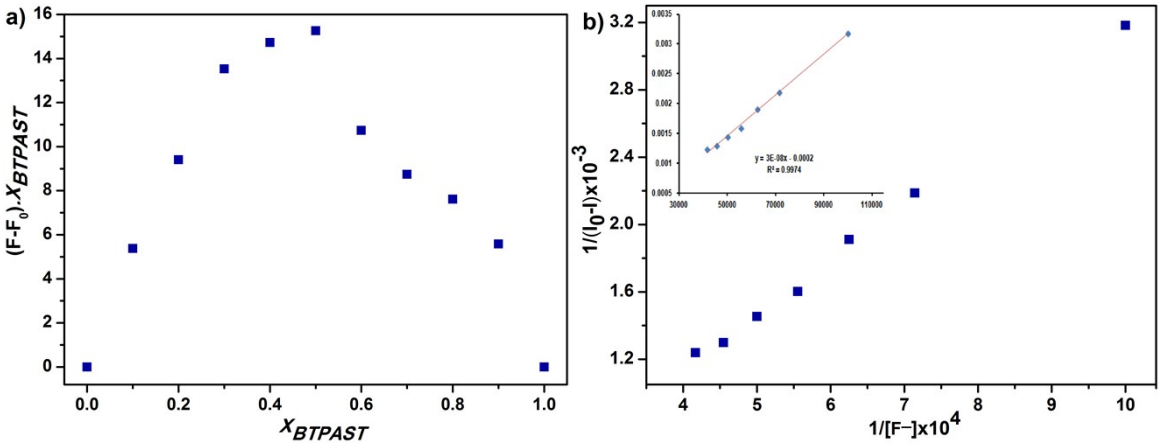

Figure S7. a) Job Plot for complexation of **BTPAST** with F^- anion; b) Benesi-Hildebrand plot of **BTPAST** by fluorescence experiments (λ = 566 nm).

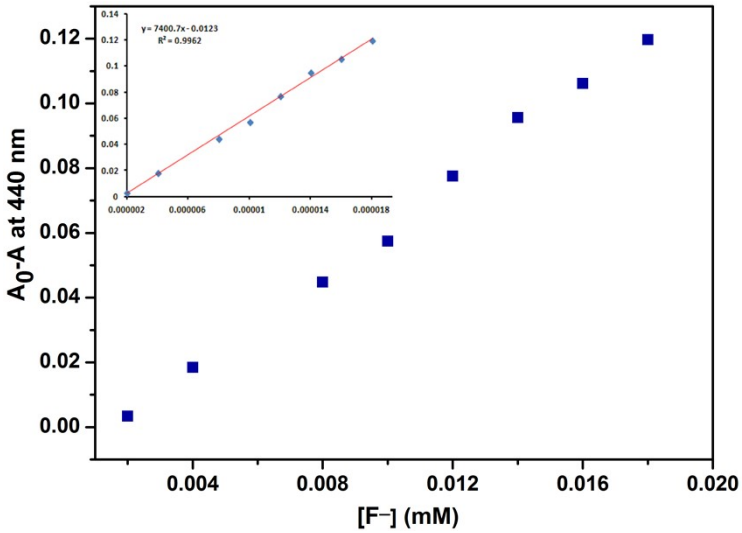

Figure S8. The absorbance changes plot of **BTPAST** (20 μM) as a function of F^- concentration in THF. [F^-] concentration: 0.002–0.018 mM (the lower concentration part).

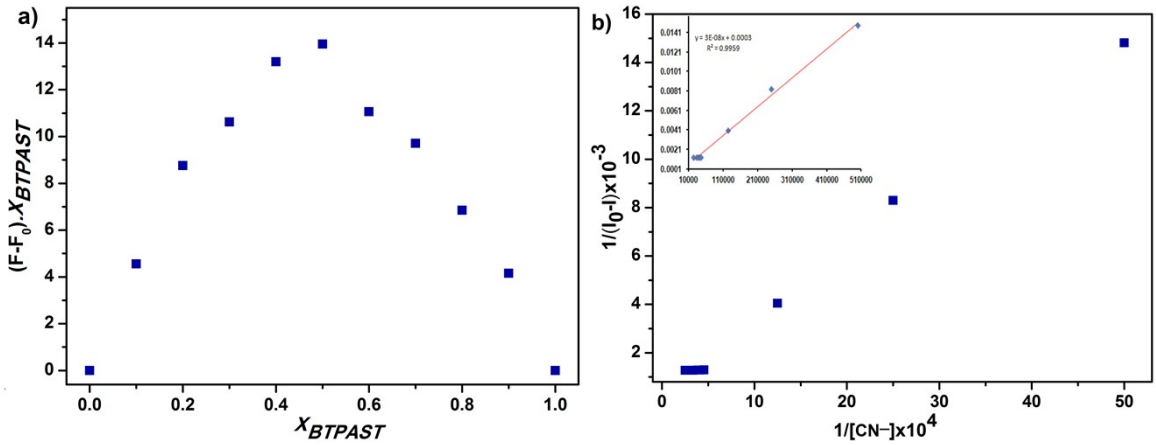

Figure S9. a) Job Plot for complexation of **BTPAST** with CN^- anion; b) Benesi-Hildebrand plot of **BTPAST** by fluorescence experiments (λ = 566 nm).

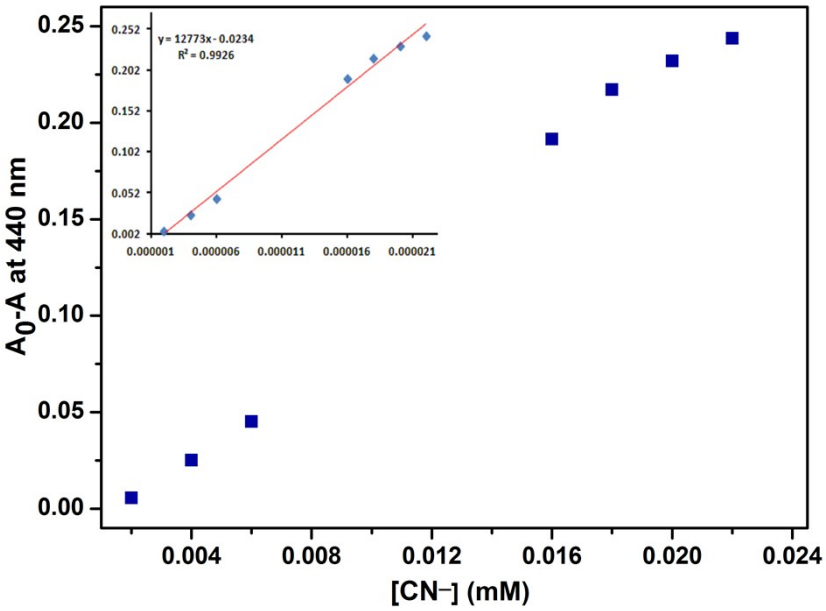

Figure S10. The absorbance changes plot of **BTPAST** (20 μM) as a function of CN^- concentration in THF. [CN^-] concentration: 0.002–0.022 mM (the lower concentration part).

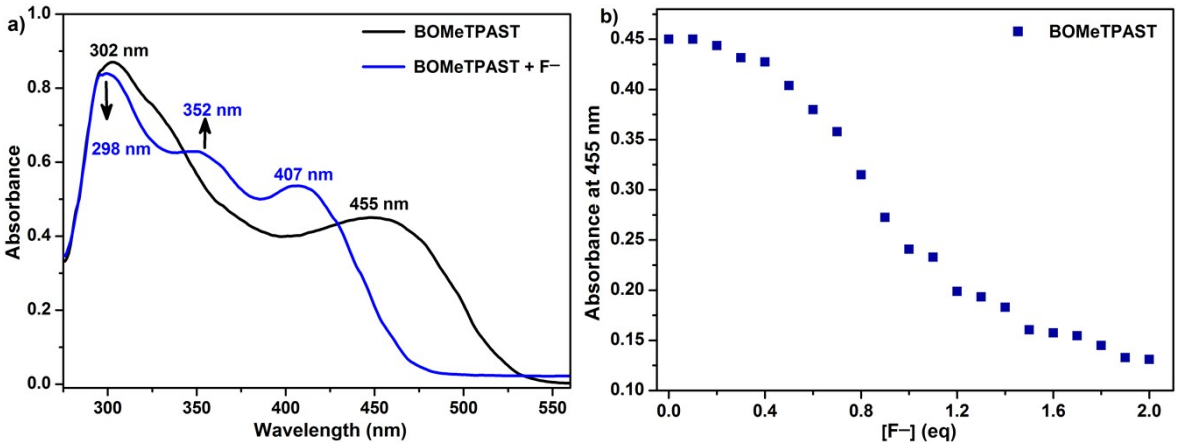

Figure S11. a) Spectral change in the absorbance of a solution **BOMeTPAST** in THF upon the addition of TBAF (0 and 2.0 eq). b) The plot of absorbance at 455 nm as a function of [F^-].

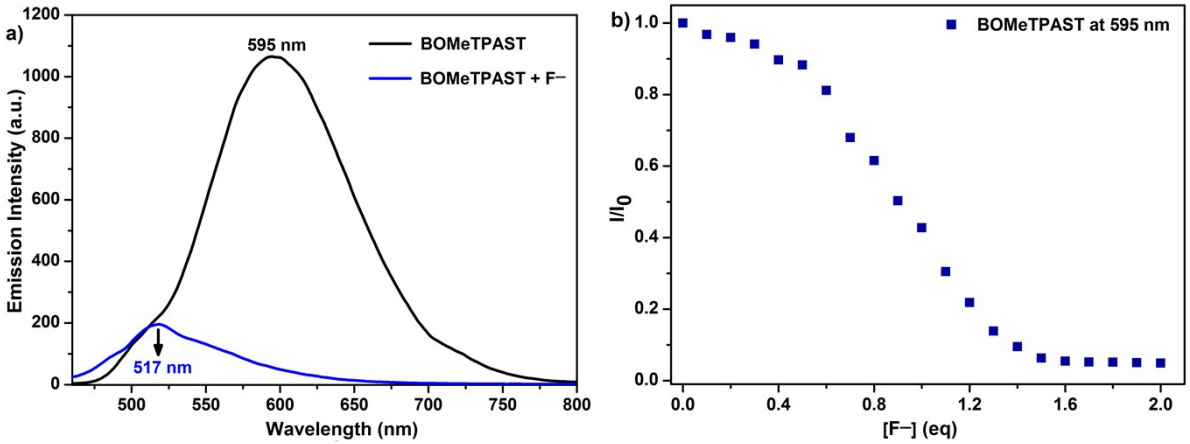

Figure S12. a) Spectral change in the emission of a solution **BOMeTPAST** in THF upon the addition of TBAF (0 and 2.0 eq) (λ_{ex} = 455 nm). b) Stern-Volmer plot of the intensity change (I_0/I) as a function of [F^-]

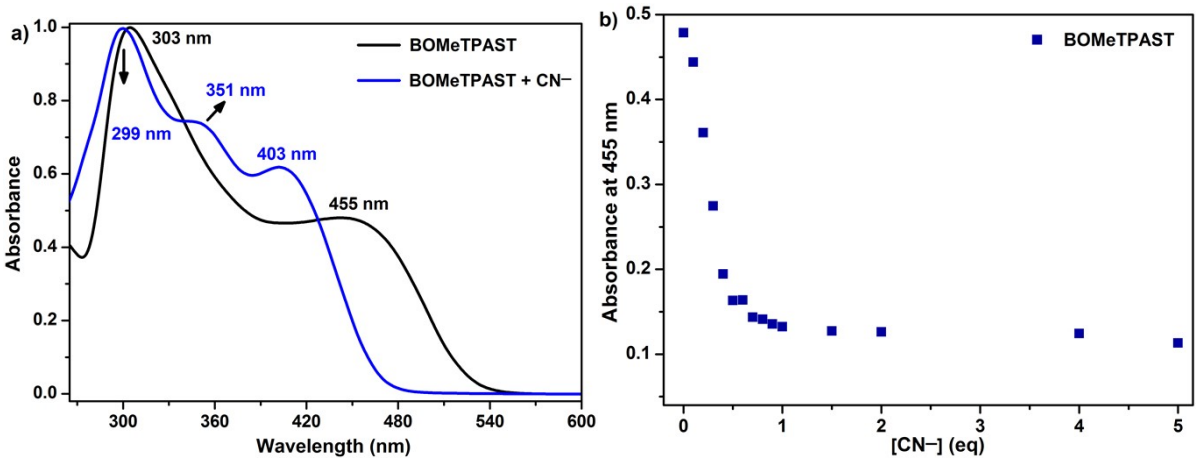

Figure S13. a) Spectral change in the absorbance of a solution **BOMeTPAST** in THF upon the addition of TBACN (0 and 5.0 eq). b) The plot of absorbance at 455 nm as a function of [CN−].

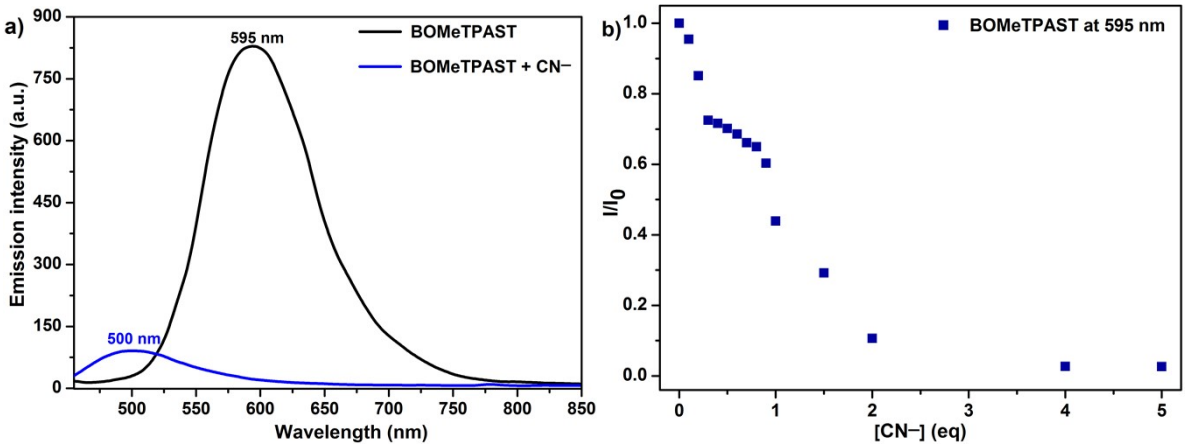

Figure S14. a) Spectral change in the emission of a solution BOMeTPAST in THF upon the addition of TBACN (0 and 5.0 eq) (λ_{ex} = 440 nm). b) Stern-Volmer plots of the intensity change (I_0/I) as a function of [CN−].

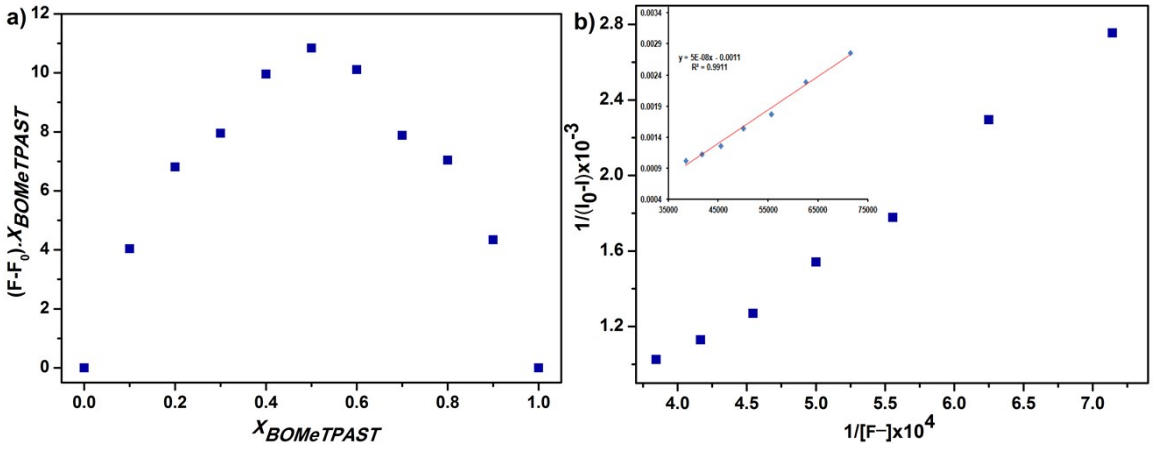

Figure S15. a) Job Plot for complexation of **BOMeTPAST** with F^- anion; b) Benesi-Hildebrand plot of **BOMeTPAST** by fluorescence experiments (λ = 595 nm).

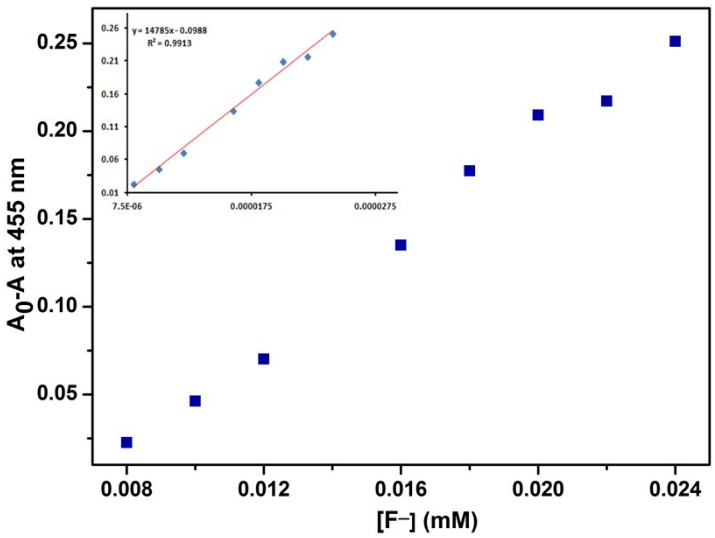

Figure S16. The absorbance changes plot of **BOMeTPAST** (20 μM) as a function of F^- concentration in THF. [F^-] concentration: 0.008–0.024 mM (the lower concentration part).

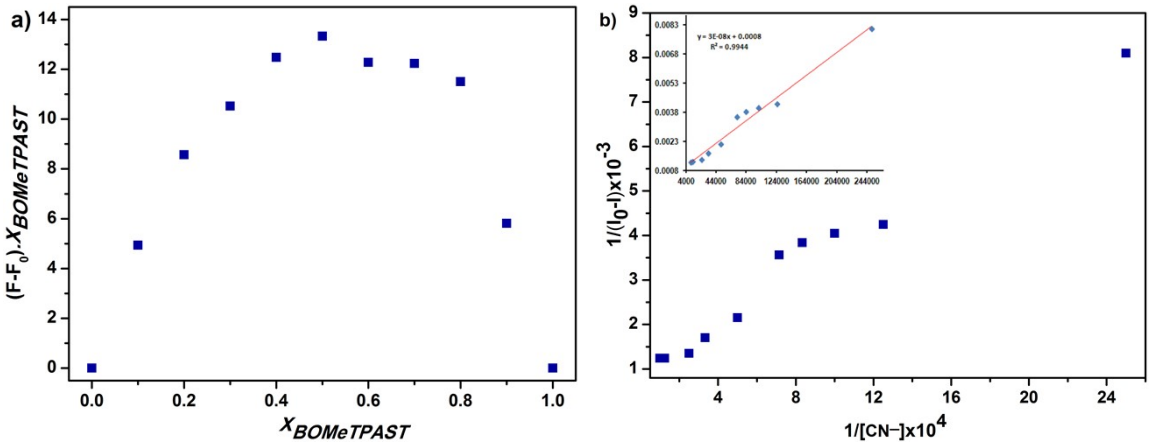

Figure S17. a) Job Plot for complexation of **BOMeTPAST** with CN^- anion; b) Benesi-Hildebrand plot of **BOMeTPAST** by fluorescence experiments (λ = 595 nm).

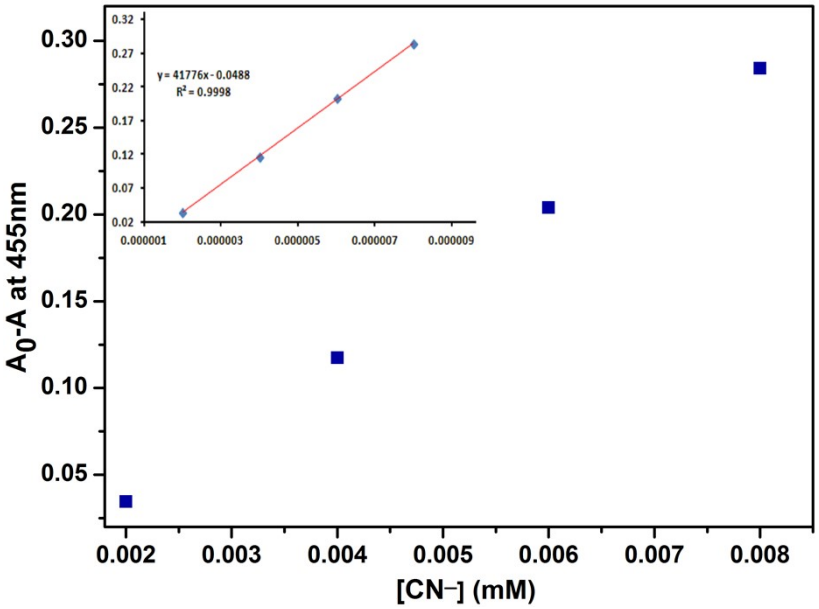

Figure S18. The absorbance changes plot of **BOMeTPAST** (20 μM) as a function of CN^- concentration in THF. [CN^-] concentration: 0.002–0.008 mM (the lower concentration part).

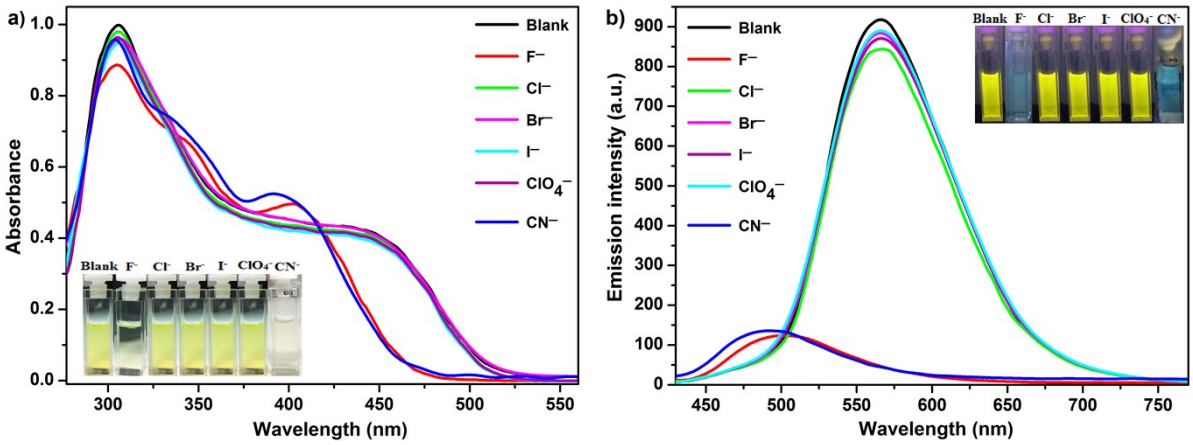

Figure S19. Change on absorption (a) and emission spectra (b) of **BTPAST** after addition of various anions (F^-, Cl^-, Br^-, I^-, CN^- and ClO_4^-) in THF, respectively. Insets: photographs of the solution under UV lamp and ambient light after different anions addition.

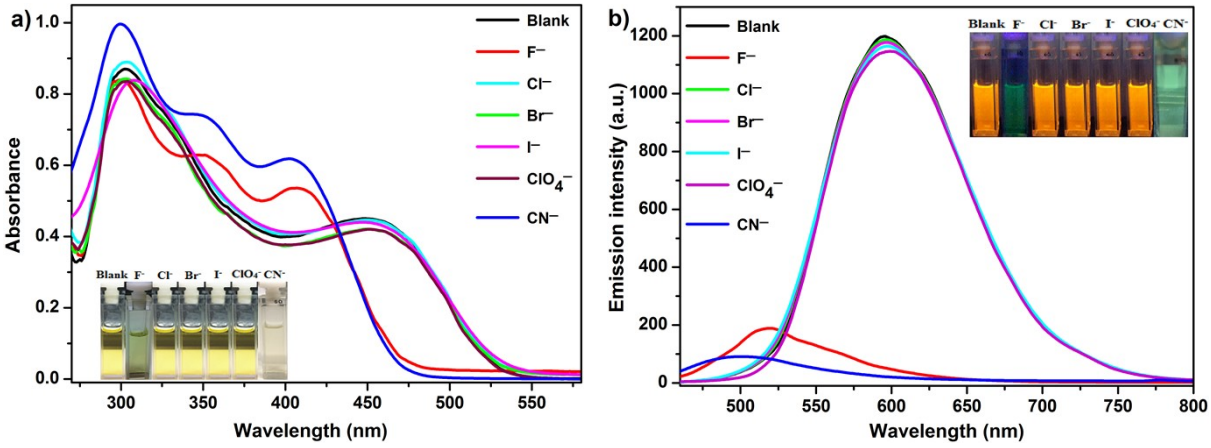

Figure S20. Change on absorption (a) and emission spectra (b) of **BOMeTPAST** after addition of various anions (F^-, Cl^-, Br^-, I^-, CN^- and ClO_4^-) in THF, respectively. Insets: photographs of the solution under UV lamp and ambient light after different anions addition.

4. NMR and MS spectra of compounds

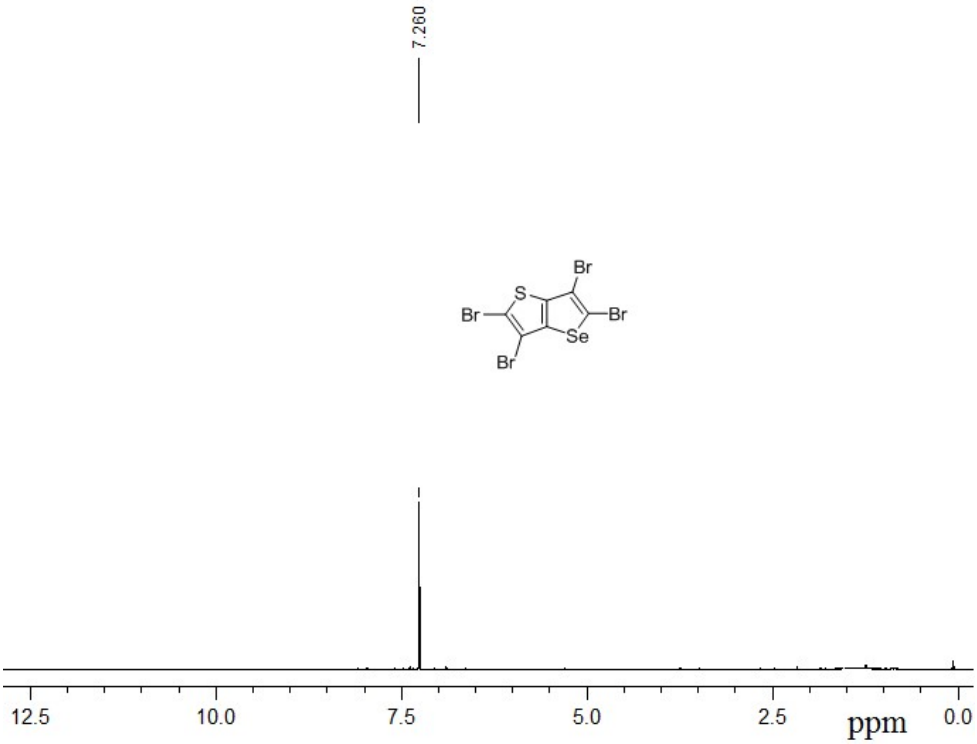

Figure S21. ^{1}H NMR (500 MHz, $CDCl_3$) spectrum of compound **2**.

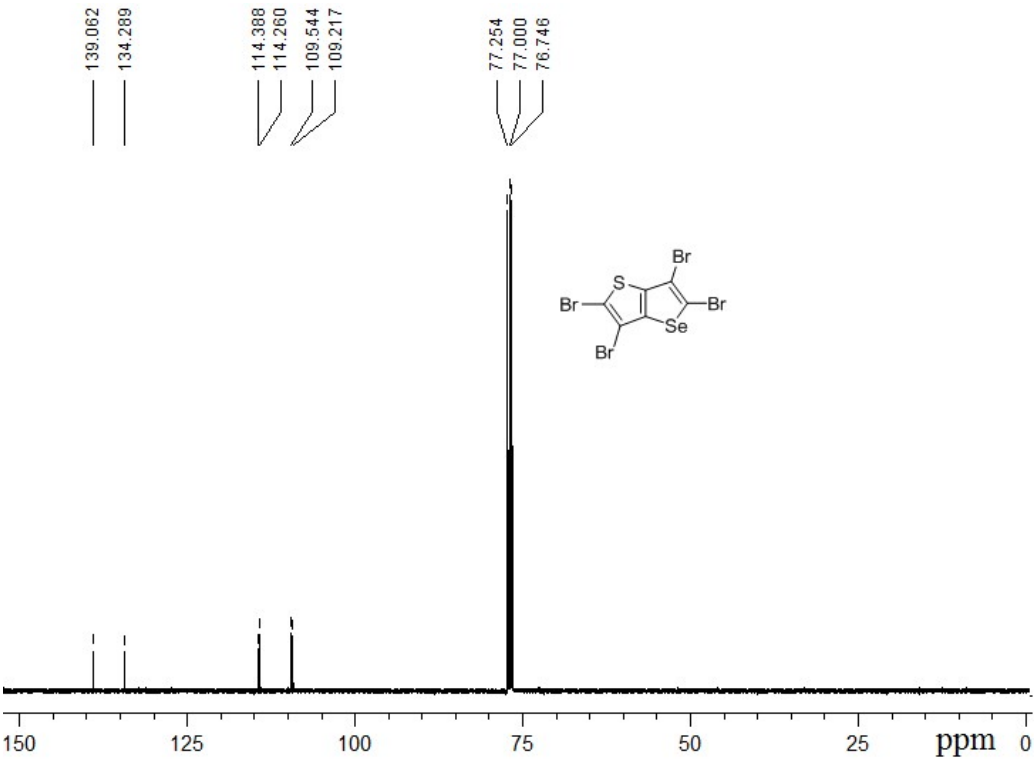

Figure S22. ^{13}C NMR (126 MHz, $CDCl_3$) spectrum of compound **2**.

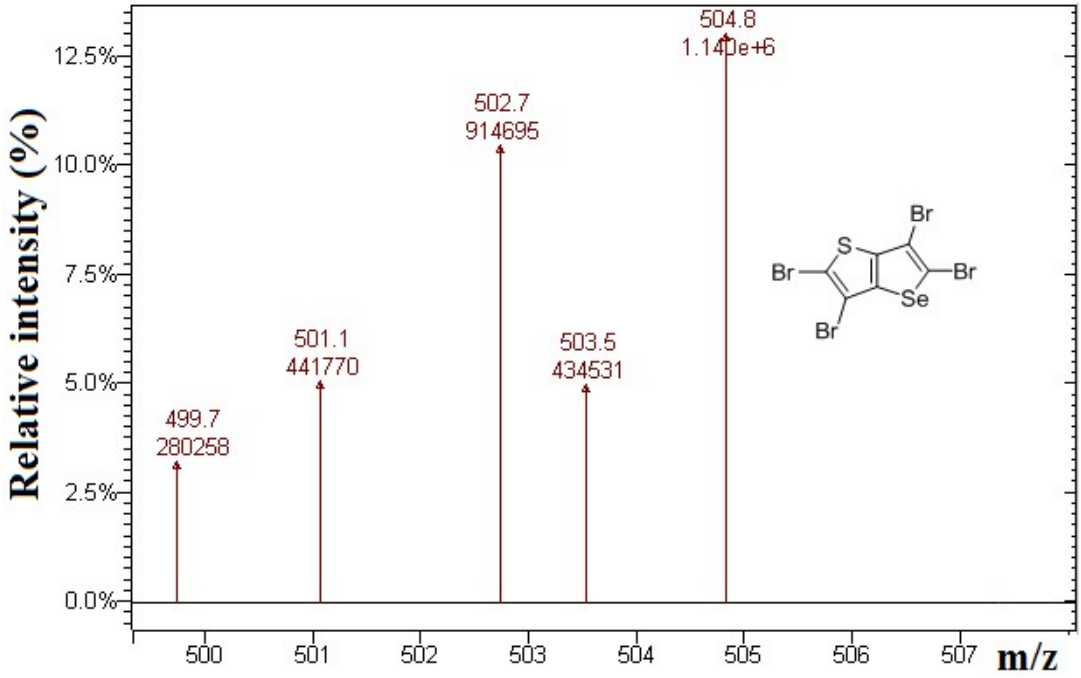

Figure S23. Mass spectrum of compound **2.**

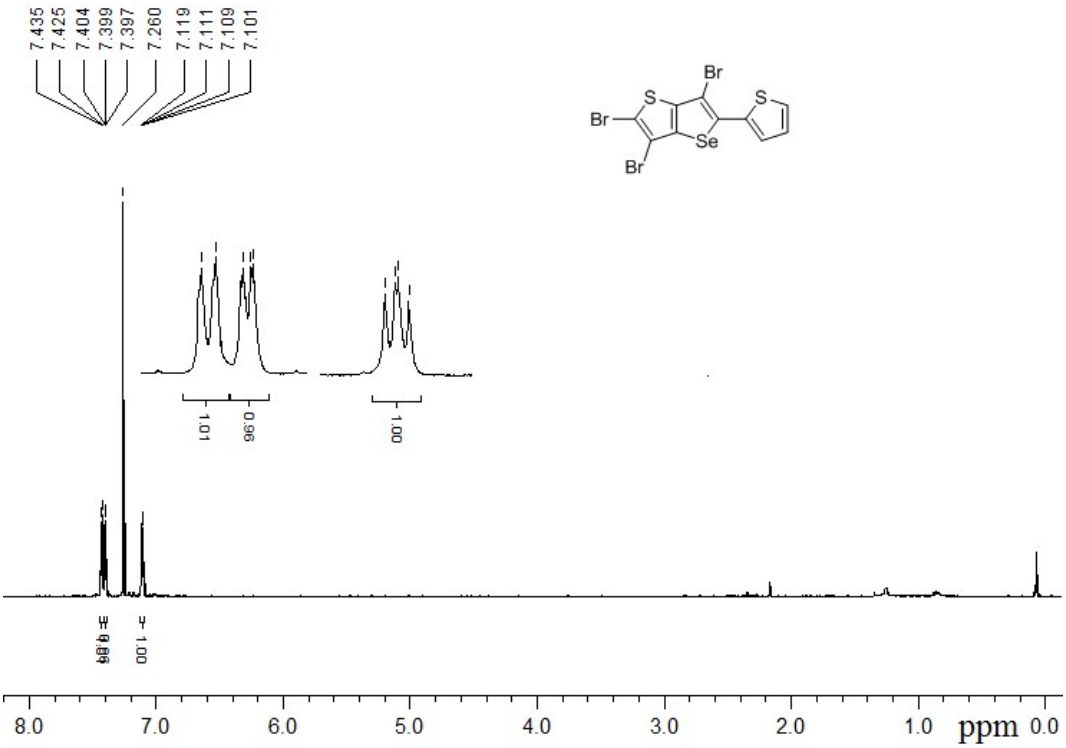

Figure S24. ^{1}H NMR (500 MHz, $CDCl_3$) spectrum of compound **3**.

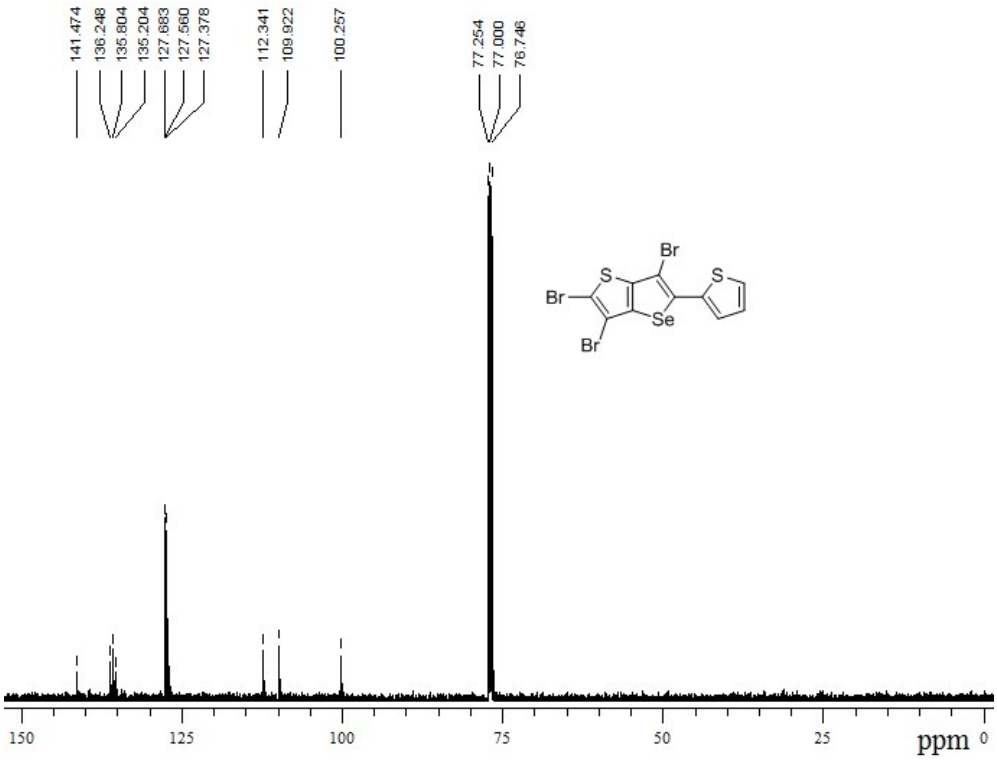

Figure S25. ^{13}C NMR (126 MHz, $CDCl_3$) spectrum of compound **3**.

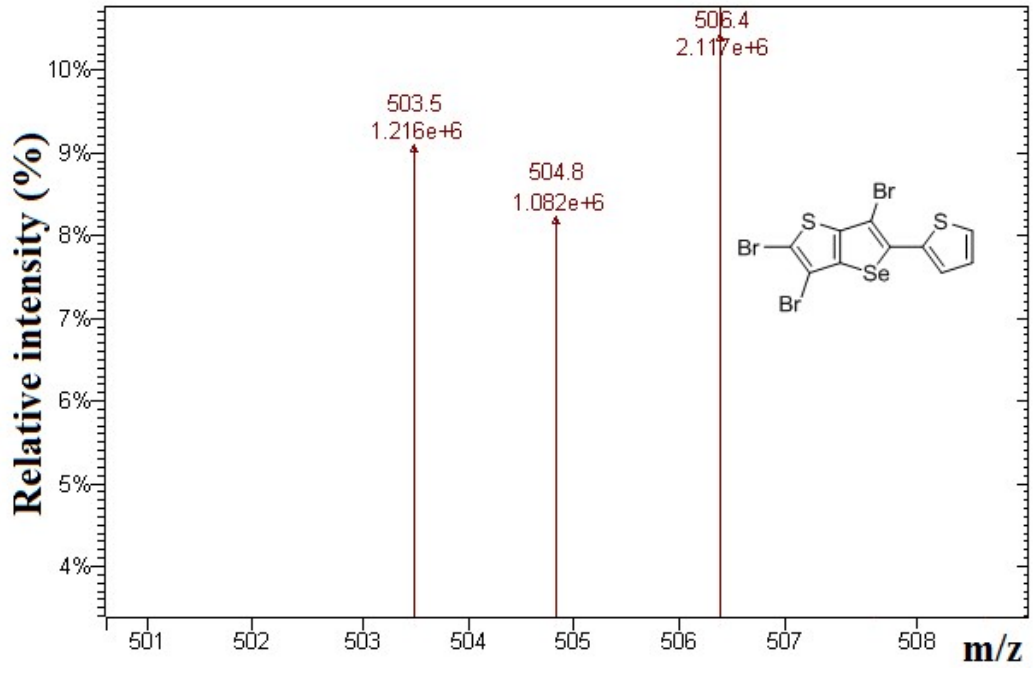

Figure S26. Mass spectrum of compound **3**.

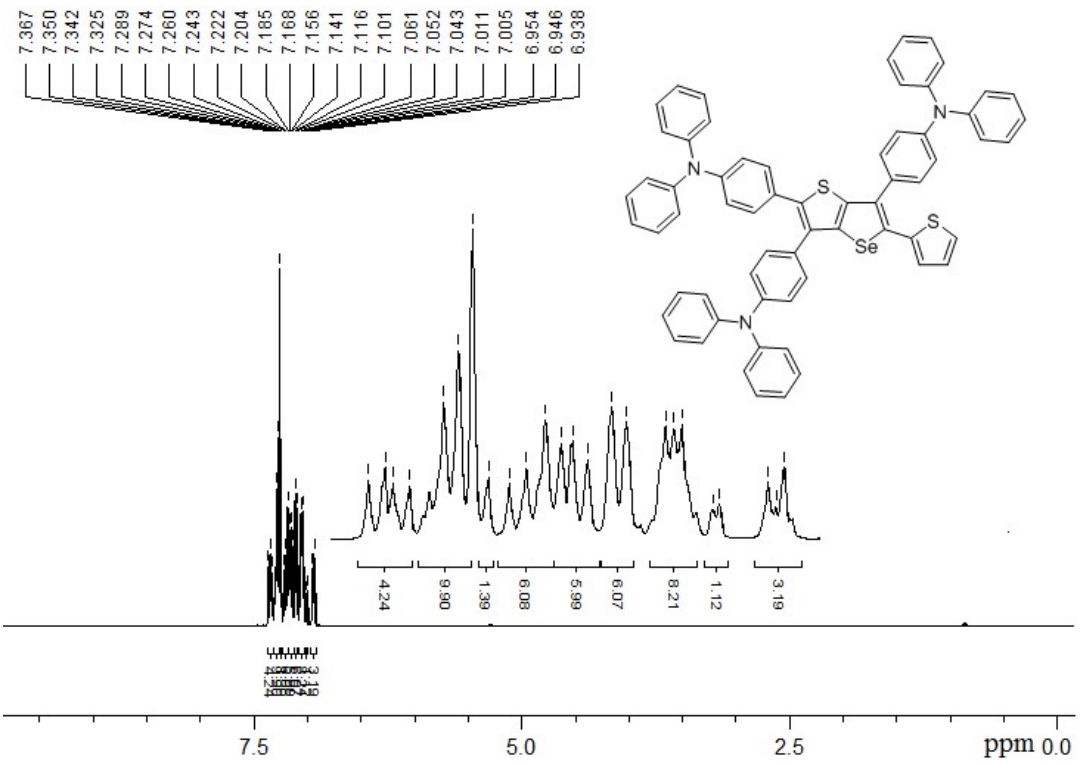

Figure S27. ^{1}H NMR (500 MHz, $CDCl_3$) spectrum of compound **TPAST**.

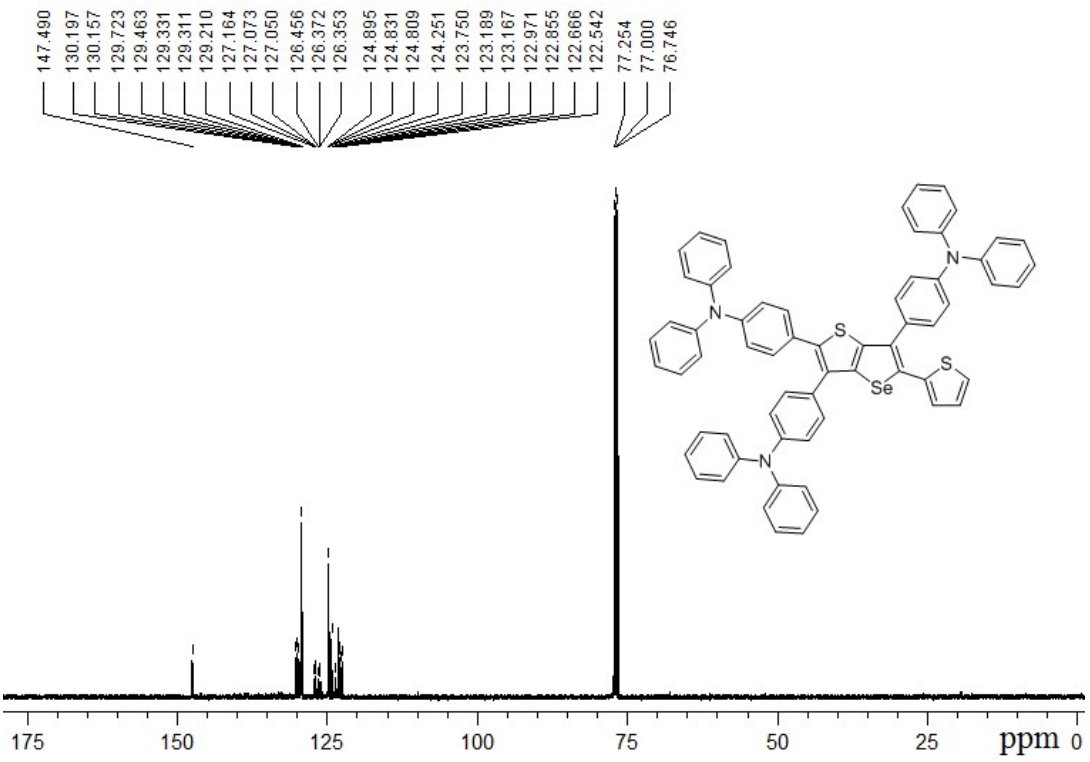

Figure S28. ^{13}C NMR (126 MHz, $CDCl_3$) spectrum of compound **TPAST**.

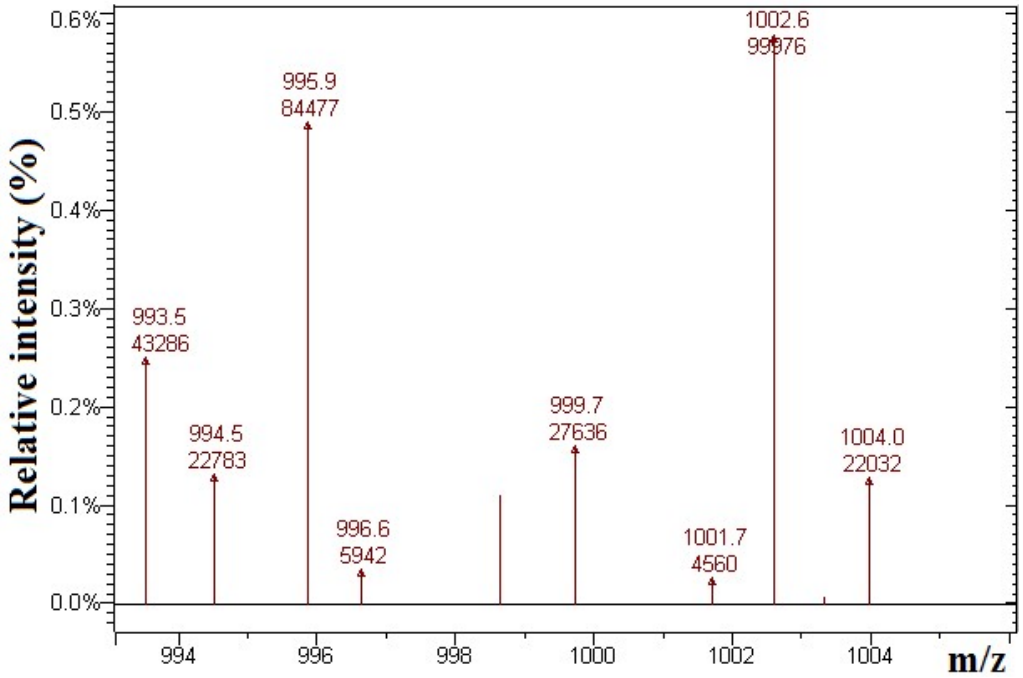

Figure S29. Mass spectrum of compound **TPAST**.

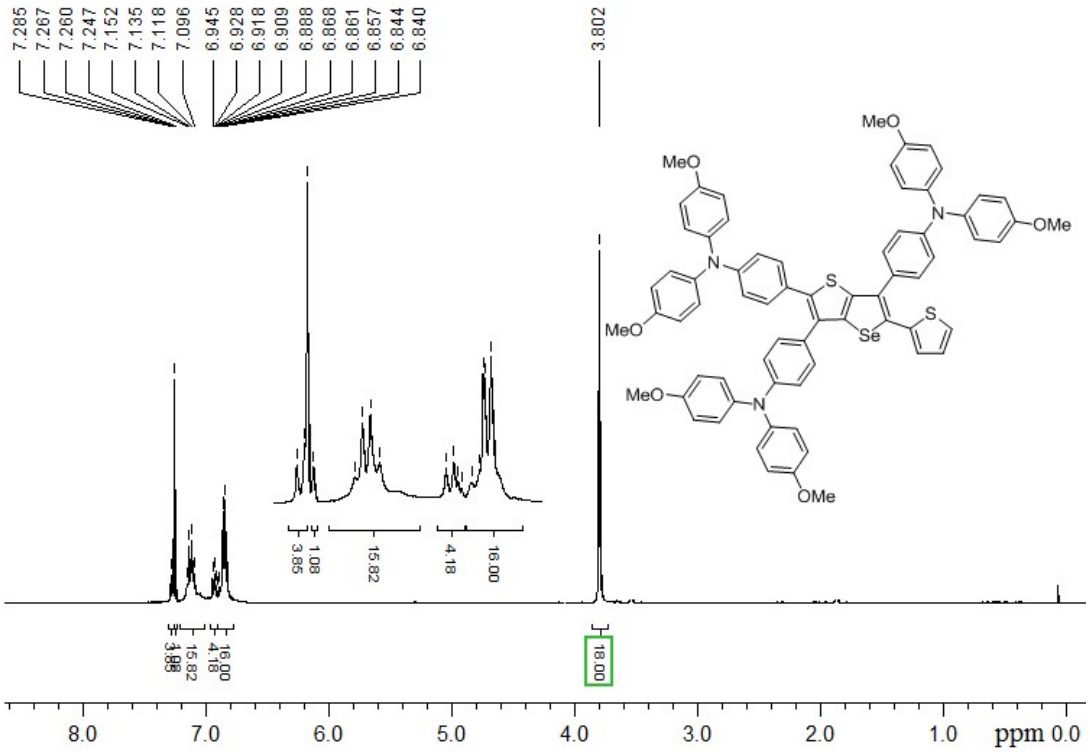

Figure S30. ^{1}H NMR (500 MHz, $CDCl_3$) spectrum of compound **OMeTPAST**.

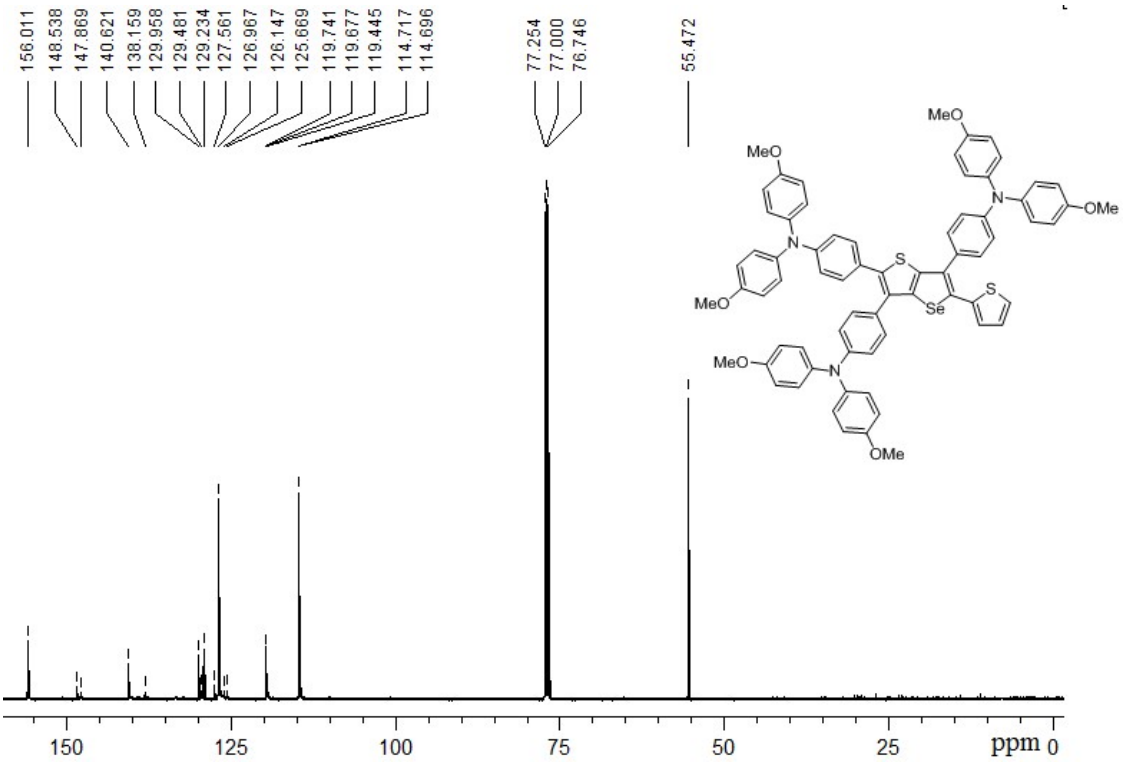

Figure S31. ^{13}C NMR (126 MHz, $CDCl_3$) spectrum of compound **OMeTPAST**.

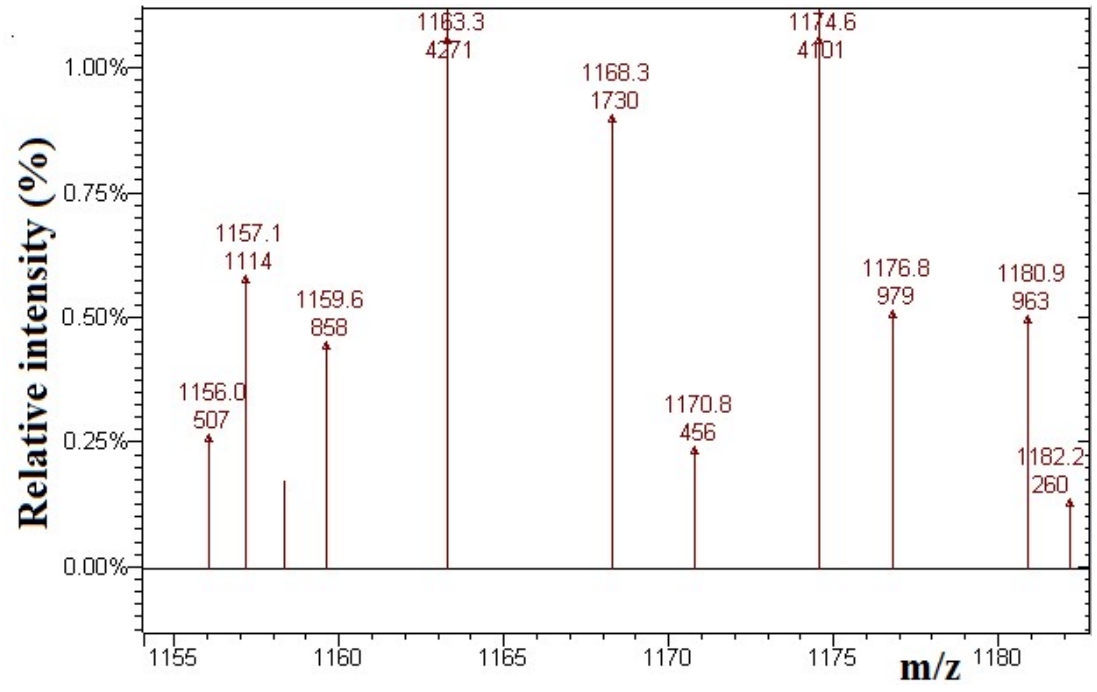

Figure S32. Mass spectrum of compound **OMeTPAST**.

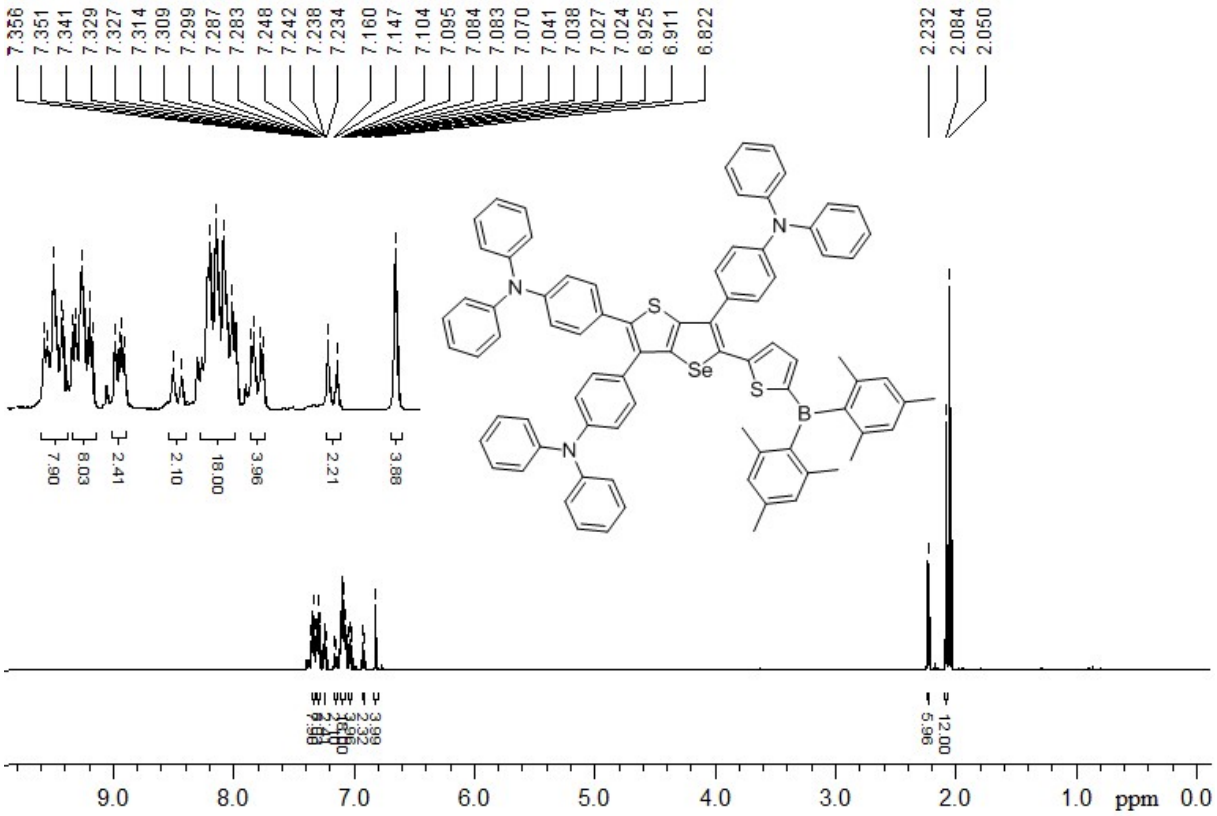

Figure S33. ^{1}H NMR (600 MHz, aseton-d_6) spectrum of compound **BTPAST**.

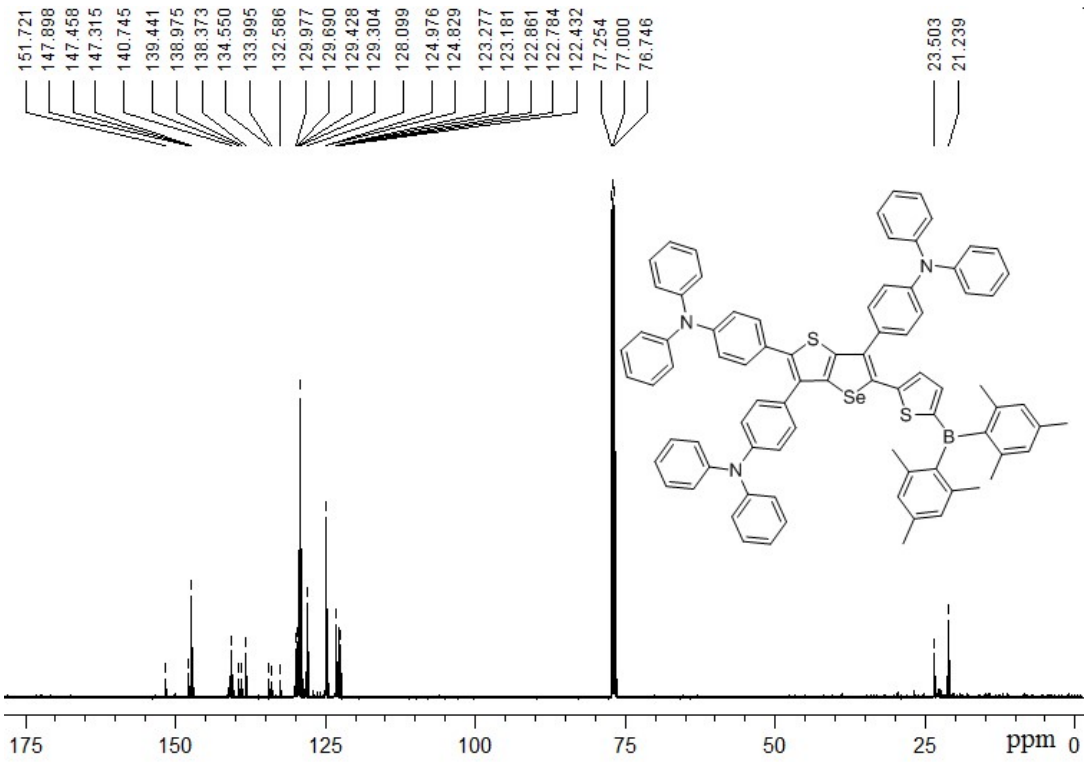

Figure S34. ^{13}C NMR (126 MHz, $CDCl_3$) spectrum of compound **BTPAST**.

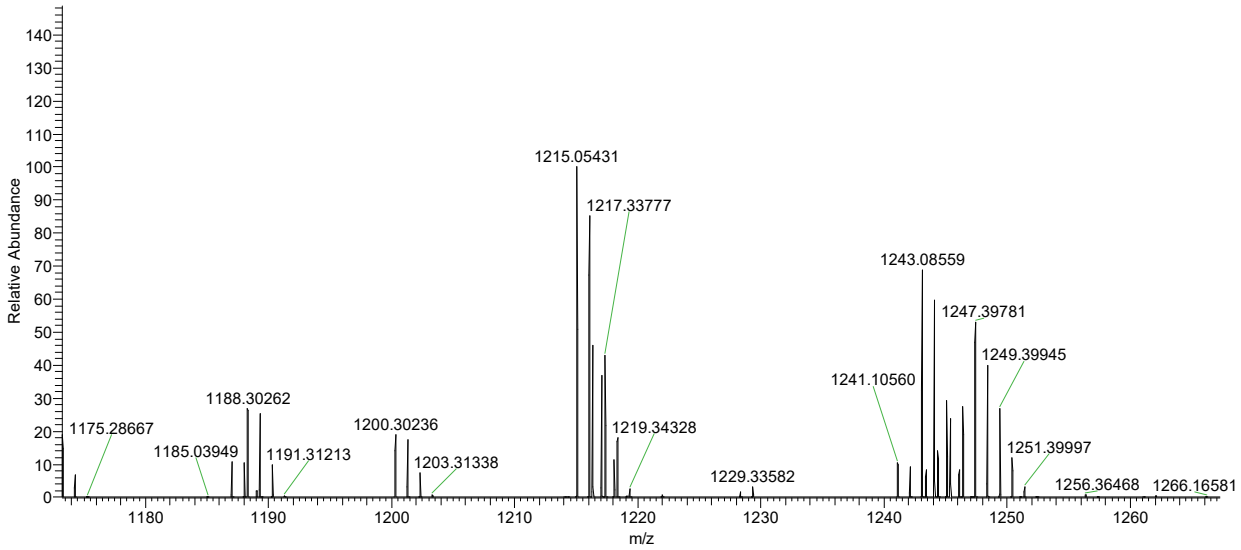

m/z	Theo. Mass	Delta (ppm)	RDB equiv.	Composition
1247.39781	1247.39509	2.18	52.0	$C_{82}H_{66}N_3BS_2Se$

Figure S35. HRMS spectrum of compound **BTPAST**.

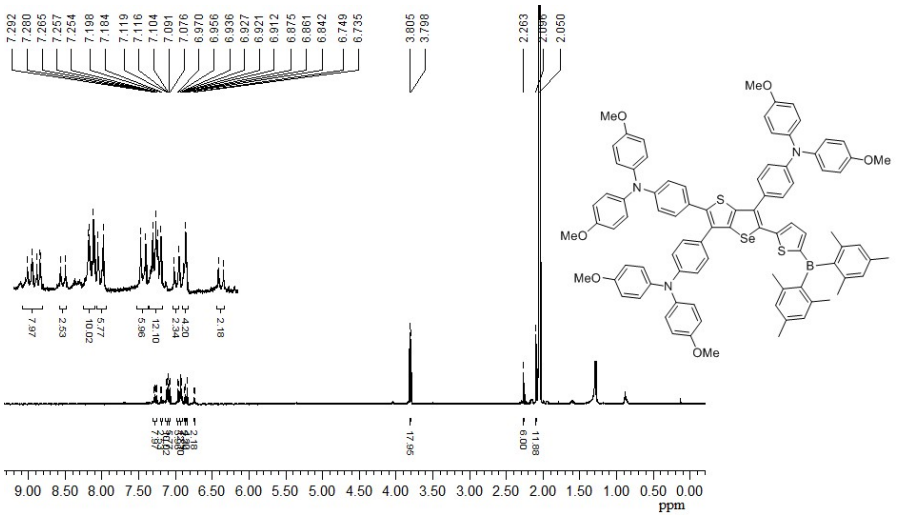

Figure S36. ^{1}H NMR (600 MHz, aseton-d_6) spectrum of compound **BOMeTPAST**.

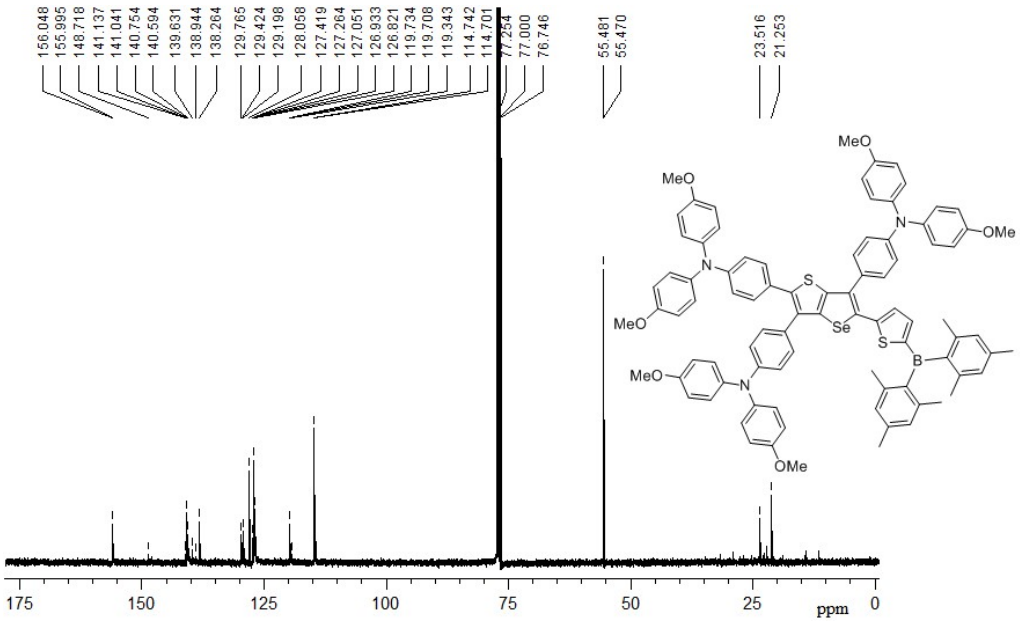

Figure S37. ^{13}C NMR (126 MHz, $CDCl_3$) spectrum of compound **BOMeTPAST**.

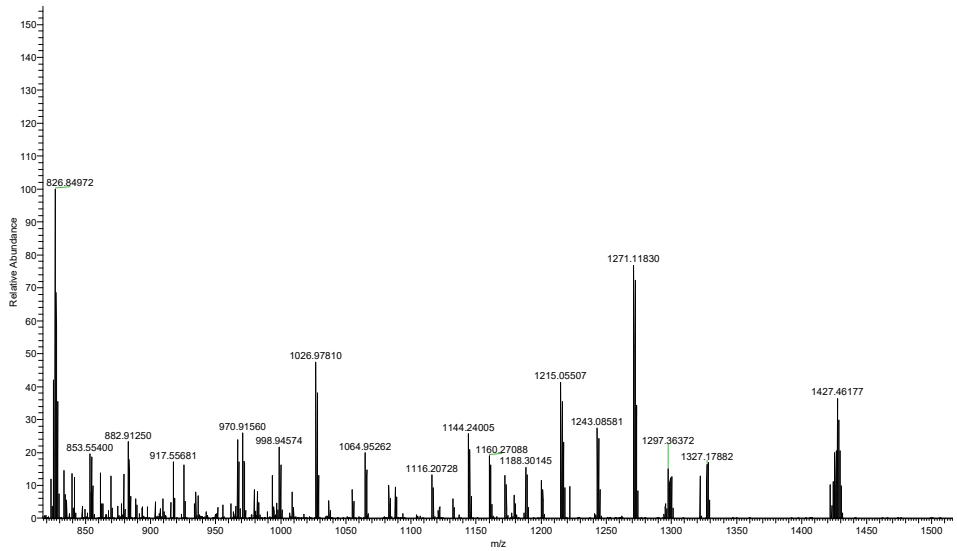

m/z	Theo. Mass	Delta (ppm)	RDB equiv.	Composition
1427.46177	1427.45848	2.30	52.0	$C_{88}H_{78}O_6N_3BS_2Se$

Figure S38. HRMS spectrum of compound **BOMeTPAST**.

References

1 C. Lo and C. Hsu, *J. Polym. Sci., Part A: Polym. Chem.* 2011, **49**, 3355−3365.

2 A. Leliege, J. Grolleau, M. Allain, P. Blanchard, D. Demeter, T. Rousseau, J. Roncali, *Chem. Eur. J.* 2013, **19**, 9948−9960.

3 L. Chen, B. Zhang, Y. Cheng, Z. Xie, L. Wang, X. Jing, F. Wang, *Adv. Funct. Mater.* 2010, **20**, 3143.

4 L. Yu, J. Xi, H.T. Chan, T. Su, L. J. Antrobus, B. Tong, Y. Dong, W. K. Chan, D. L. Phillips, *J. Phys. Chem. C* 2013, **117**, 2041.
5 G. Turkoglu, *Org. Commun.* 2018, **11**, 12-22.
6 G. Turkoglu, M. E. Cinar and T. Ozturk, *RSC Adv.* 2017, **7**, 23197–23207.
7 P. Sakthivel, K. Sekar, G. Sivaraman, S. Singaravadivel, G. Anbud, and G. S. Kumar, *Applied Organometallic Chemistry,* 2020, **34**, 1-9.
8 H. A. Benesi, J. H. Hildebrand, H. Benesi, J. A. Hildebrand, *J Am Chem Soc* 1949, **71**, 2703–2707.
9 Z. Li, S. Wang, L. Xiao, X. Li, X. Shao, X. Jing, X. Peng, L. Ren, *Inorganica Chimica Acta* 2018, **476**, 7-11.
10 G. Li, Y. Zhao, J. Li, J. Cao, J. Zhu, X. Sun, Q. Zhang, *J Org Chem* 2015, **80**, 196-203.